ISSN 0023-1584, Kinetics and Catalysis, 2011, Vol. 52, No. 6, pp. 809–816. © Pleiades Publishing, Ltd., 2011.
Original Russian Text © A.N. Murashkevich, O.A. Alisienok, I.M. Zharskii, 2011, published in Kinetika i Kataliz, 2011, Vol. 52, No. 6, pp. 830–837.

# Physicochemical and Photocatalytic Properties of Nanosized Titanium Dioxide Deposited on Silicon Dioxide Microspheres

**A. N. Murashkevich*, O. A. Alisienok, and I. M. Zharskii**

*Belarusian State Technological University, Minsk, 220050 Belarus*

** e-mail: man@bstu.unibel.by*

Received December 23, 2010

**Abstract**—The synthesis of $SiO_2$ core–$TiO_2$ shell composites from a titanium dioxide sol and a suspension of microspherical silicon dioxide is described. The main factors ensuring the formation of a composite with a preset morphology are the size and charge of the $TiO_2$ sol particles (10–45 nm) and silicon dioxide core particles (300–700 nm), the pH values of the suspensions of the starting components and the resulting composite, and the proportions and way of mixing of the silicon- and titanium-containing components. The $SiO_2$ core–$TiO_2$ shell composites show high photocatalytic activity in the degradation of Rhodamine FL-BM dye (rate constant of $k = 0.0813$ min$^{-1}$) and are much more active than precipitated $TiO_2$ powder ($k = 0.0022$ min$^{-1}$). The activity of the composite is determined by the calcination temperature (700–800°C), by the proportion and accessibility of the active component ($TiO_2$), and by the presence of a dopant ($P_2O_5$).

**DOI:** 10.1134/S0023158411060140

Photocatalytic processes are attracting increasing interest because they can help solve a variety of problems, including those of decomposition of hazardous and colored organic compounds in solutions and gases [1–6], debacterization [7], creation of nanophotonic and sensor devices [8, 9], intensification of organic synthesis processes [10–13], and hydrogen production [14, 15]. The most popular photocatalyst is titanium dioxide, for it has high photocatalytic activity and chemical stability and is inexpensive and nontoxic [16–19]. However, photocatalyst processes employing pure titanium dioxide are difficult to carry out in practice because, at elevated temperatures, this compound undergoes phase transitions changing its particle size, while use of finely divided titanium dioxide, including as a hydrosol, in real processes is limited by the fact that the catalyst nanoparticles are difficult to separate from the substrate. Numerous attempts have been made to fix titanium dioxide on the surface of various supports, such as glass spheres and fiber [20, 21] and zeolites [22]. When preparing such composites, it is essential to preserve the high catalytic activity of titanium dioxide and the possibility of manifestation of quantum size effects and to choose an appropriate support.

Among the binary oxide-based catalytic systems, of great interest are nanosized silicon and titanium dioxides and related materials, which can be obtained as a variety of structural and morphological modifications, namely, aerogels, xerogels, coagels, coprecipitated powders, mesostructured substances, core–shell composites, nanotubes, and related nanostructures [23–26]. Since heterogeneous catalytic reactions take place on the catalyst surface, core–shell composites have the following advantages over coprecipitated composites: They allow their textural and adsorption properties to be varied in a wider range owing to the independent formation of the core and shell [27–29]. They allow the crystallization of the titanium-containing component to be controlled. It is possible to prepare monodisperse samples with a preset particle size. This is particularly important when the composites are used as precursors of photonic crystals. In heterogeneous catalytic applications, this makes it easier to separate the catalyst from the substrate for catalyst reuse [30–33].

With a catalyst core consisting of silicon dioxide, whose morphological, structural, adsorption, and surface properties can fairly readily be controlled by varying the synthesis conditions and the nature of the starting components, it is possible to obtain chemically stable and nontoxic photocatalysts with preset properties.

Here, we report the effects of the initial substances (silicon dioxide serving as the catalyst core and $TiO_2$ sol) and synthesis conditions (proportions of the components in the composite, pH of the dispersion medium at all synthesis stages, and calcination temperature) on the physicochemical and photocatalytic properties of nanosized titanium dioxide deposited on silicon dioxide microspheres.

## EXPERIMENTAL

### *Materials*

Microspherical silicon dioxide to be used as the catalyst core was precipitated from aqueous solutions of sodium silicate ($SiO_2/Na_2O = 2.4$) with a solution of ammonium carbonate or acetate and ammonia.

Alternatively, microspherical silicon dioxide was precipitated from water–ethanol solutions of tetraethoxysilane (TEOS) by a modified Stober method using dodecylamine as the template. By varying initial synthesis conditions and employing the structure-forming agent, it was possible to vary the specific surface area of the core between 180 and 700 $m^2/g$ and to control the particle size in the 300–700 nm range [34].

For preparing a $TiO_2$ sol, titanium dioxide was precipitated with ammonium carbonate from a vigorously stirred titanium tetrachloride solution with pH 6 or lower. The precipitate was filtered, washed until free of chloride ions, and then peptized with nitric acid (H/Ti = 0.2–0.8, 1.5–6 wt % $TiO_2$) [35].

The formation of a composite with the given morphology is largely due to the Coulomb interaction between particles bearing opposite charges and differing in their size. $TiO_2$ sol particles 10–45 nm in size, which are positively charged at pH <6, are attracted by larger (300–700 nm), negatively charged particles of silicon dioxide to form a shell on the latter. The deposition of nanosized titanium dioxide onto silicon dioxide microspheres takes place mainly via heteroadagulation. Titanium dioxide sol was introduced into a silicon dioxide suspension (pH 1.0–1.5), and aqueous ammonia was added under vigorous stirring to bring the dispersion medium to pH 3–5. The resulting solid was filtered, washed with distilled water until neutral pH, dried at 120°C, and heat-treated at 300–1000°C.

The composite was doped by introducing nitrogen-containing components (urea, thiourea, or diethylamine) into the synthesis. A modifying aqueous solution of phosphoric acid (0.5–5 wt % in terms of $P_2O_5$) was added to the samples before heat treatment.

### *Characterization of Materials*

The $TiO_2$ content of the materials was measured photocolorimetrically [36]. The textural and adsorption properties of the materials were determined by adsorption gravimetry using nitrogen or phenol dissolved in *n*-heptane as the adsorbate. The specific surface area of the $TiO_2$ shell of the composite was estimated from the specific surface area of the core and that of the composite as a whole using the additivity rule. X-ray diffraction patterns were obtained on a DRON-3 diffractometer (Ni-filtered Cu$K_\alpha$ radiation) at room temperature in the $2\theta = 11°–70°$ range at a scanning rate of 2 deg/min. The amount of crystalline titanium-containing component in the heat-treated material was determined by the acid dissolution method based on the difference between the solubilities of crystalline and amorphous $TiO_2$ in sulfuric acid [37]. Composite samples were placed in a 1 M sulfuric acid solution and were held there for 12 h. Thereafter, the titanium dioxide that had passed into solution was quantified in the filtrate by photocolorimetry.

The morphology of silicon dioxide and composite particles was studied using a JEOL JSM 5610 LV scanning electron microscope. The isoelectric point (pI) was determined by measuring the electrokinetic potential by the macroelectrophoresis method at various pH values of the composite suspension without a supporting electrolyte. The electrical properties of the surface were used to estimate the morphology of the composite. The similarity between the surface electrical properties of the $SiO_2$ core–$TiO_2$ shell composite and pure titanium dioxide (pI 6) made it possible to identify the composite with the desired morphology and to determine the extent to which the silicon dioxide core is screened by the titanium dioxide shell.

### *Photocatalytic Activity Measurements*

The photocatalytic activity of the composites was measured in the degradation of Rhodamine FL-BM dye under the action of UV radiation without focusing on intermediate degradation products. The commercial dye was used as received. The source of UV radiation was a DRSh 250-3 ultrahigh-pressure mercury lamp. The initial dye concentration was $10^{-5}$ mol/l, and the photocatalyst concentration was $10^{-3}$ wt %. Photocatalytic activity was evaluated as the decrease in the dye concentration during the process. To do this, the reaction mixture was sampled at intervals, the catalyst was separated out, and the extinction coefficient of the samples was measured on a KFK-3 photocolorimeter at a wavelength of 566 nm, which corresponds to the absorbance maximum of the dye. Rate constants were calculated under the assumption that the dye degradation reaction is first-order. This assumption is confirmed by extensive experimental data on the degradation of organic dyes, including Rhodamine, in the presence of irradiated titanium dioxide [30, 38, 39].

## RESULTS AND DISCUSSION

We attempted to see how the particle size and surface electrical properties of the composite and of its $TiO_2$ shell depend on some initial catalyst synthesis conditions (size, morphology, and charge of the silicon dioxide particles and $TiO_2$ sol), on some variable synthesis parameters (pH values of the suspensions of the starting components and the resulting composite), on the proportions of the starting components, and on the way they were combined. For this purpose, we carried out four series of experiments on the synthesis of $SiO_2$ core–$TiO_2$ shell composites, systematically varying one of the above parameters while maintaining the other conditions invariable. The results of these experiments are presented in Table 1.

An analysis of these results suggests that the $TiO_2$ sol particles that have the smallest statistical mean diameter *d* (Table 1, entry 1) form a uniform shell on the surface of the $SiO_2$ particles, as is indicated by the fact that the pI of the composite is close to the pI of titanium dioxide (pI 6). An increase in the mean effec-

**Table 1.** Effect of synthesis conditions on the most important properties of the $SiO_2$ core–$TiO_2$ shell composite

| Entry | Synthesis conditions[a] | | | | | | Properties of the composite | | | |
|---|---|---|---|---|---|---|---|---|---|---|
| | $TiO_2$ content of the $TiO_2$–$HNO_3$ mixture, wt % | $d_{TiO_2}$, nm | pH of the $TiO_2$ sol | $S_{sp}$ of $SiO_2$, $m^2/g$ | pH of the $SiO_2$ suspension | Deposition pH | pI | $TiO_2$ content, % | $S_{sp}$[b], $m^2/g$ | |
| | | | | | | | | | composite | shell |
| Effect of the particle size of the $TiO_2$ sol | | | | | | | | | | |
| 1 | 3 | 10 | 0.8 | 197 | 1.5 | 4.0 | 4.8 | 26.5 | 266 (377[c]) | 457 |
| 2 | | 24 | 0.7 | | 1.8 | 3.5 | 3.8 | 29.6 | 262 | 364 |
| 3 | | 42 | 0.8 | | 1.5 | 4.0 | 3.5 | 29.9 | 275 | 458 |
| Effect of the deposition pH | | | | | | | | | | |
| 4 | 1.5 | 13 | 1.2 | 182 | 1.5 | 3.0 | 5.2 | 26.2 | 191 | 216 |
| 5 | | | 1.2 | | 1.5 | 3.7 | 3.8 | 28.3 | 223 | 327 |
| 6 | | | 1.2 | | 1.5 | 4.2 | 4.6 | 27.4 | 204 | 262 |
| 7 | | | 1.2 | | 1.5 | 5.6 | 5.9 | 27.8 | 242 | 398 |
| Effect of the $TiO_2$ content | | | | | | | | | | |
| 8 | 3 | 12 | 0.9 | 189 | 1.5 | 4.5 | 4.3 | 8.2 | 119 | – |
| 9 | | | 0.8 | | 1.5 | 4.4 | 5.4 | 18.4 | 165 | 59 |
| 10 | | | 0.9 | | 1.5 | 4.8 | 4.8 | 25.4 | 220 | 311 |
| 11 | | | 0.8 | | 1.5 | 4.5 | 5.3 | 32.8 | 185 | 177 |
| 12 | | | 0.7 | | 1.5 | 4.8 | 3.7 | 44.6 | 192 | 196 |
| Effect of the textural and adsorption properties of the core | | | | | | | | | | |
| 13 | 1.5 | 12 | 0.9 | 182 | 1.5 | 4.7 | 4.8 | 25.4 | 220 | 311 |
| 14 | | | 1.0 | 268 | 0.7 | 4.8 | 4.8 | 29.6 | 366 | 711 |
| 15 | | | 0.8 | 677[d] | 1.5 | 4.7 | 4.8 | 22.1 | 445 (503[c]) | – |

[a] For the synthesis conditions, see EXPERIMENTAL. The H/Ti ratio at the final stage of $TiO_2$ sol preparation is 0.8.
[b] Specific surface areas were determined by phenol adsorption from *n*-heptane solution.
[c] Specific surface area determined by nitrogen adsorption.
[d] $SiO_2$ core prepared by the modified Stober method.

tive diameter of the $TiO_2$ sol particles is favorable for the formation of a more porous shell and, accordingly, for a stronger effect of the core on the surface electrical properties of the composite. This effect manifests itself as a shift of pI to smaller pH values (Table 1, entries 2, 3).

At a suspension acidity of pH ≤3, the formation of the necessary structure apparently does not take place. The silicon dioxide surface in this pH range has a near-zero charge ($SiO_2$ has pI 2.0–2.5). This is unfavorable for the Coulomb interaction between the components. In addition, the product obtain in this pH range is difficult to filter. On the whole, the specific surface area of the composite increases with an increasing deposition pH. The same trend was observed earlier in the precipitation of pure titanium dioxide [34]. However, raising the pH of the dispersion medium leads to the formation of a less porous shell structure, as is indicated by the pI of the composite being very close to the pI of titanium dioxide (Table 1, entry 7).

At low titanium dioxide contents, the specific surface area of the composite is smaller than the $S_{sp}$ of the $SiO_2$ core. This is due to titanium dioxide filling pores in, and spaces between, core particles (Table 1, entries 8, 9). This effect may be rather useful in preparing a composite in which the amorphous silicon dioxide matrix contains $TiO_2$ nanocrystallites whose size is determined by then pore size or interparticle spaces in silicon dioxide. The optimum $TiO_2$ content of the core–shell composite is within the 20–40 wt % range, and its precise value is application-dependent.

By increasing the specific surface area of the core from 182 to 677 $m^2/g$, it is possible to obtain a shell with a still more developed surface unnatural of pure titanium dioxide precipitated from solution under the same conditions, whose maximum specific surface area is 200–300 $m^2/g$. The increase in $S_{sp}$ is not accompanied by any significant change in the pI of the composite. This can be due to the constancy of the $TiO_2$ content of the composite and to the similarity of the composite synthesis conditions.

The silicon dioxide particles obtained from water–ethanol solutions of TEOS are more monodisperse and less aggregated than the product obtained from sodium silicate solutions (Fig. 1). This may be due to the polymeric structure of the silicate anion in the sodium silicate solutions, which imparts some specific

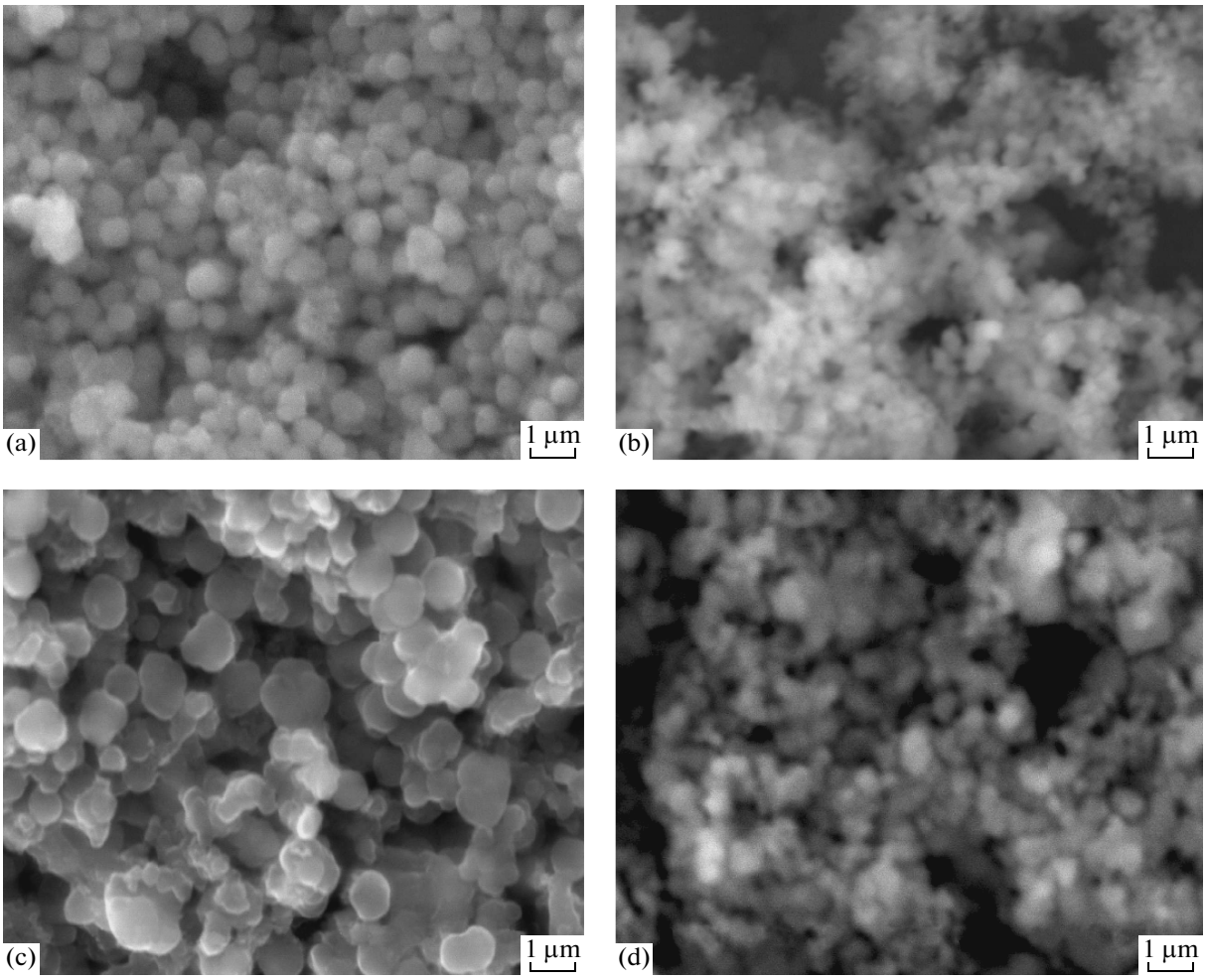


**Fig. 1.** Micrographs of (a, b) silicon dioxide obtained from (a) TEOS and (b) sodium silicate and (c, d) $SiO_2$ core–$TiO_2$ shell composites with cores prepared from (c) TEOS and (d) sodium silicate.

features to the hydrolysis process and to the subsequent structure formation stages. The growth of the composite particles without changes in their shape is evidence of the formation of a product with the desired core–shell morphology.

According to our data, the specific surface area of the titanium dioxide shell and that of the composite as a whole increase with an increasing degree of dispersion of the core (Table 1, entries 13–15). However, the silicon dioxide core prepared by the modified Stober method has not only a large specific surface area, but also a considerable proportion of micropores (Fig. 2), and, as a consequence, the textural and sorption characteristics (specific surface area and pore volume) of the composite are worse than those of the core because of micropore blocking by nanosized colloidal particles of the titanium dioxide sol. A comparison between the photocatalytic activities of $SiO_2$ core–$TiO_2$ shell samples differing in the degree of dispersion of the core verifies this hypothesis. As is demonstrated in Fig. 3, the sample with a $SiO_2$ core prepared by the modified Stober method, which has a considerably larger specific surface area, is less active. This is likely due to the fact that titanium dioxide in this sample is less accessible to the activating radiation and to the reaction medium.

The X-ray diffraction patterns of the $SiO_2$ core–$TiO_2$ shell composite with $SiO_2/TiO_2 = 70 : 30$ heat-treated in the 120–1000°C range for 10 h (Fig. 4) indicate that even heat treatment at 300°C causes the formation of the anatase phase, whose content increases as the temperature is raised to 700°C. Above 800°C, anatase gradually turns into almost pure rutile, the most stable $TiO_2$ phase, whose proportion increases rapidly as the temperature is further raised. The presence of silicon dioxide in the coprecipitated $SiO_2$–$TiO_2$ composite markedly hampers the crystallization of the titanium-containing component during heat treatment [40]. This is believed to be due to the possibility of isomorphic substitution of titanium for silicon in the silicon–oxygen tetrahedra with the formation of Si–O–Ti bonds. The crystallization of $TiO_2$ in the

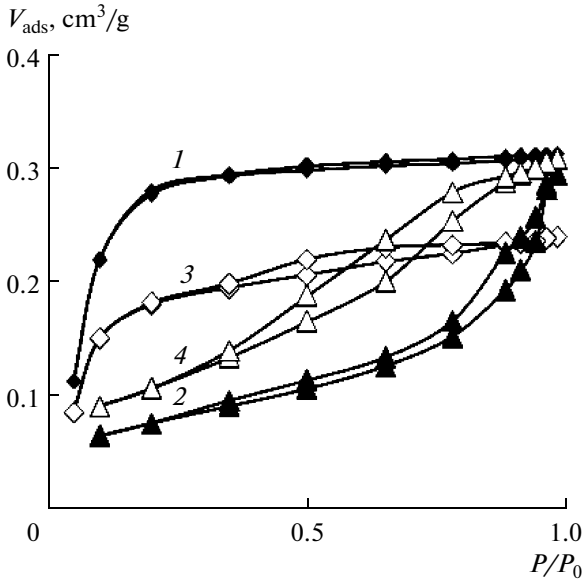


**Fig. 2.** Nitrogen adsorption–desorption isotherms for (*1*, *2*) $SiO_2$ obtained (*1*) by the modified Stober method and (*2*) from a sodium silicate solution and (*3*, *4*) the composites prepared using these silicon dioxide samples, respectively.

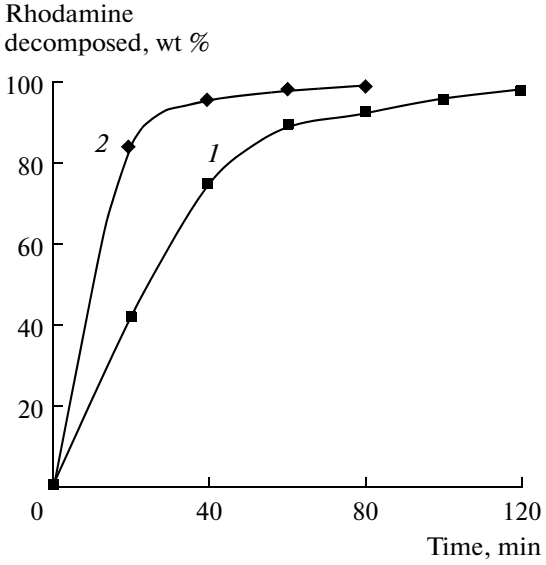


**Fig. 3.** Photocatalytic activity of $SiO_2$ core–$TiO_2$ shell composites whose $SiO_2$ core is prepared (*1*) by the modified Stober method and (*2*) from a sodium silicate solution.

$SiO_2$ core–$TiO_2$ shell composite also proceeds much less rapidly than in the case of pure titanium dioxide, in which the anatase-to-rutile transition takes place already at 600–700°C (Fig. 4).

Raising the titanium dioxide content of the composite from 10 to 30 wt % leads to an increase in the degree of crystallinity of the titanium-containing component upon heat treatment, and this manifests itself as a higher photocatalytic activity of the product (Figs. 5, 6). The lower activity of the composite containing 40 wt % $TiO_2$ is likely explained by the fact that, with an increasing titanium dioxide content, the properties of the titanium dioxide shell get closer to the properties of pure titania: the structure becomes

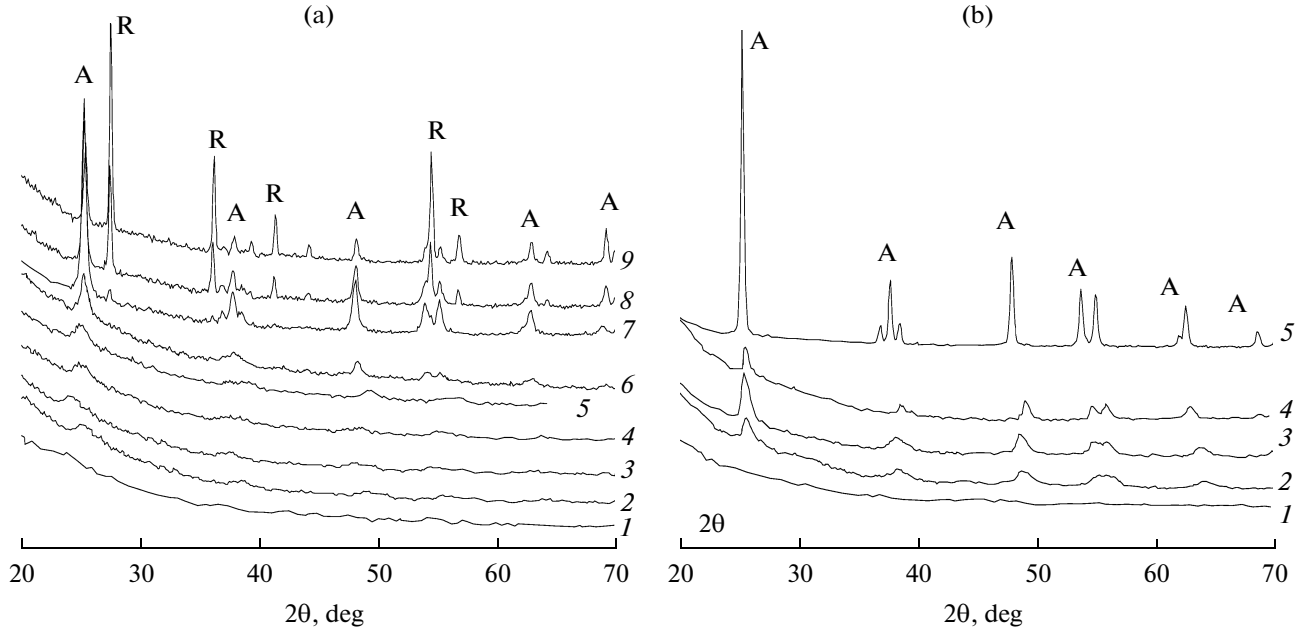


**Fig. 4.** X-ray diffraction patterns of (a) $SiO_2$ core–$TiO_2$ shell composite ($SiO_2/TiO_2$ = 70/30) and (b) pure titanium dioxide, both calcined at (*1*) 120, (*2*) 300, (*3*) 400, (*4*) 500, (*5*) 600, (*6*) 700, (*7*) 800, (*8*) 900, and (*9*) 1000°C. A = anatase; R = rutile.

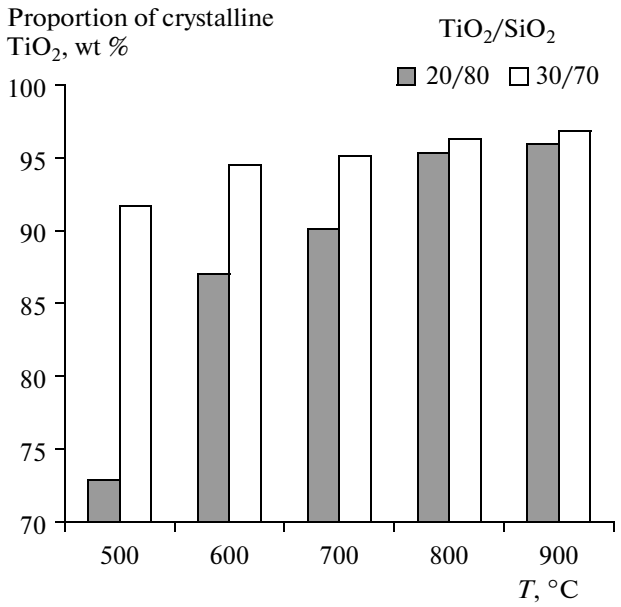


**Fig. 5.** Effect of the composition of the composite on the crystallization of the titanium-containing component during heat treatment.

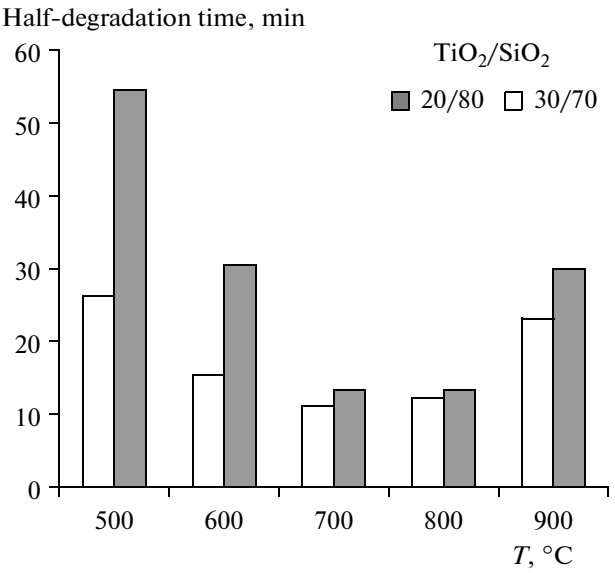


**Fig. 7.** Effect of heat-treatment temperature on the the photocatalytic activity of $SiO_2$ core–$TiO_2$ shell composites with different proportions of the components.

thermally less stable, which leads to the conversion of anatase into rutile, a less active phase.

The highest photocatalytic activity in Rhodamine FL-BM degradation is shown by the composite containing 30 wt % $TiO_2$, calcined at 700°C (Fig. 7). As the calcination temperature is further elevated, the activity of this composite decreases because of anatase recrystallization into rutile and because of the marked decrease in the specific surface area. The composites containing 20 wt % $TiO_2$ retain their high photocatalytic activity after calcination in a wider temperature range (up to 700–800°C). This is due to the slowdown of the recrystallization and polymorphic transformation of the titanium dioxide shell owing to the stronger effect of the silicon dioxide core on this process.

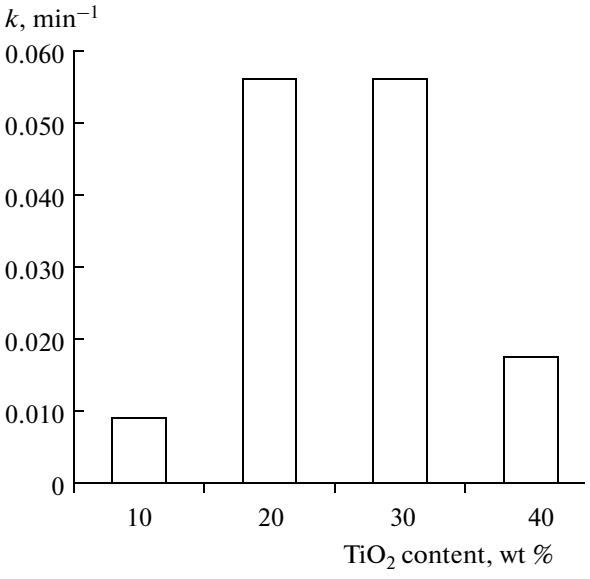


**Fig. 6.** Rate constant of Rhodamine FL-BM degradation on the $TiO_2$ content of the $SiO_2$ core–$TiO_2$ shell composite calcined at 700°C.

The introduction of nitrogen, sulfur, or phosphorus as their compounds into the composite enhances the photocatalytic activity of the titanium-containing component (Fig. 8). In the general case, this effect is due to the appearance of impurity levels in the band gap of titanium dioxide. This reduces the energy necessary for photogeneration of an electron–hole pair to be involved in the oxidation and, accordingly, destruction of organic compounds [41].

The photocatalytic degradation of Rhodamine FL-BM on phosphorus-doped composites proceeds in some cases at a higher rate than the same process on the undoped composite (Table 2). However, it is inappropriate to increase the dopant content above 0.5 wt % because this causes the formation of titanium phosphates, which slow down $TiO_2$ crystallization [42]. This is indicated by the fact that the photocatalytic activity peak of the phosphorus-doped composites is shifted to higher calcination temperatures.

A comparison between the photocatalytic activity of the $SiO_2$ core–$TiO_2$ shell composite and that of pure titanium dioxide suggests that the morphological features and surface properties of the composite, as well as the structural state of the titanium-containing component (which is determined by the synthesis and heat treatment conditions), are favorable for more rapid

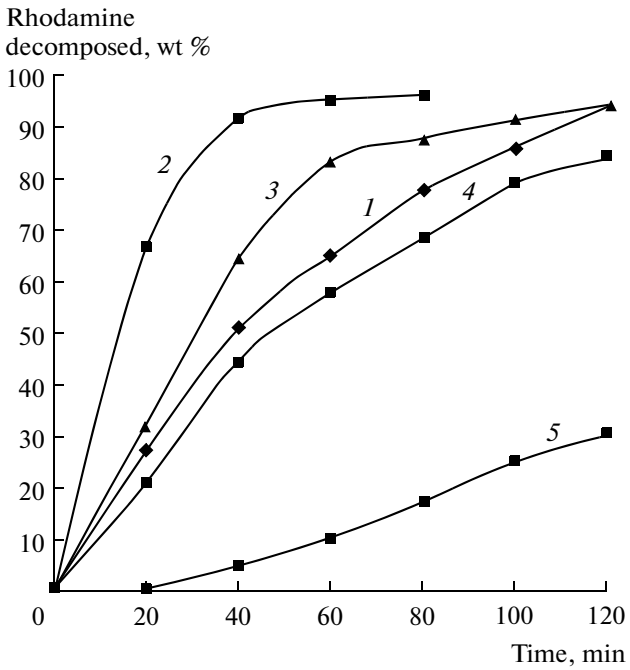


**Fig. 8.** Photocatalytic activity of $SiO_2$ core–$TiO_2$ shell composites ($SiO_2/TiO_2 = 70/30$, calcination temperature of 700°C) doped with (*1*) thiourea, (*2*) phosphoric acid, and (*3*) diethylamine and that of (*4*) undoped composite and (*5*) pure $TiO_2$.

Rhodamine FL-BM degradation (for the composite, $k = 0.0813$ min$^{-1}$; for precipitated $TiO_2$ powder, $k = 0.0022$ min$^{-1}$). A certain contribution to the photocatalytic activity of the composite can be made by the surface of the silicon dioxide core at the dye adsorption stage.

Thus, the main factors determining the formation of the $SiO_2$ core–$TiO_2$ shell composites are the size and charge of the titanium dioxide sol and silicon dioxide core, the pH of the dispersion medium of the initial components, the pH of the resulting suspension, and the proportions of the components in the composite. The $SiO_2$ core–$TiO_2$ shell composites show high photocatalytic activity in the degradation of Rhodamine FL-BM dye. Their activity depends on the calcination temperature, the percentage and accessibility of the catalytic component, and the presence of a dopant.

**Table 2.** Rate constants for Rhodamine FL-BM degradation in the presence of $SiO_2$ core–$TiO_2$ shell photocatalysts ($SiO_2/TiO_2 = 70/30$) doped with phosphoric acid

| Calcination temperature, °C | $P_2O_5$ content, wt % | | | |
|---|---|---|---|---|
| | 0 | 0.5 | 2 | 5 |
| 600 | 0.0314 | 0.0454 | 0.0322 | 0.0281 |
| 700 | 0.0557 | 0.062 | 0.046 | 0.0264 |
| 800 | 0.0552 | 0.0813 | 0.0449 | 0.0466 |
| 900 | 0.0502 | 0.0401 | 0.032 | 0.0202 |

## REFERENCES


1. Aguado, J., Grieken, R., Lopez-Munoz, M.-J., and Marugan, J., *Appl. Catal.*, 2006, vol. 312, p. 202.
2. Mohamed, M.M., Solama, T.M., and Yamaguchi, T., *Colloids Surf., A*, 2002, vol. 207, p. 25.
3. Soboleva, N.M., Nosonovich, A.A., and Goncharuk, V.V., *Khim. Tekhnol. Vody*, 2007, vol. 29, p. 125.
4. Aiqin Zhang, Rongbin Zhang, Ning Zhang, Sanguo Hong, and Ming Zhang, *Kinet. Catal.,* 2010, vol. 51, p. 529.
5. Shi, J., Zheng, J., Hu, Y., and Zhao, Yu., *Kinet. Catal.*, 2008, vol. 49, p. 279.
6. Nikazar, M., Golivand, K., and Makhanpur, K., *Kinet. Catal.*, 2007, vol. 48, p. 214.
7. Khoroshikh, V.M. and Belous, V.A., *Fiz. Inzh. Poverkhn.*, 2009, vol. 7, p. 223.
8. Jenn-Feng, L., Chuin-Shan, C., Bang-Ying, Y., and Wen-Cheng, J.W., *J. Am. Ceram. Soc.*, 2006, vol. 89, p. 1257.
9. Koyamaw, H., Fujimoto, M., Ohno, T., Suzuki, H., and Tanaka, J., *J. Am. Ceram. Soc.*, 2006, vol. 89, p. 3536.
10. Hadi Nur, *Mater. Sci. Eng., B*, 2006, vol. 133, p. 49.
11. Kholdeeva, O.A., Trukhan, N.N., Vanina, M.P., Romannikov, V.N., Parmon, V.N., Mrowiec-Bialon, J., and Jarzebski, A.B., *Catal. Today*, 2002, vol. 75, p. 203.
12. Beck, C., Mallat, T., Burgi, T., and Baiker, A., *J. Catal.*, 2001, vol. 204, p. 428.
13. Müller, C.A., Schneider, M.S., Mallat, T., and Baiker, A., *J. Catal.*, 2000, vol. 192, p. 448.

14. Yiliang, L., Liejin, G., Wei, Y., and Hongtan, L., *J. Power Sources*, 2006, vol. 150, p. 1300.
15. Vorontsov, A.V., Kozlova, E.A., Besov, A.S., Kozlov, D.V., Kiselev, S.A., and Safatov, A.S., *Kinet. Catal.*, 2010, vol. 51, p. 801.
16. Inagaki, M., Nakazawa, Y., Hirano, M., Kobayashi, Y., and Toyoda, M., *Int. J. Inorg. Mater.*, 2001, vol. 3, p. 809.
17. Yan, H. and Chunwei, Y., *J. Cryst. Growth*, 2005, vol. 274, p. 563.
18. Aguado, J., Grieken, R., Lopez-Munoz, M.-J., and Marugan, J., *Appl. Catal.*, 2006, vol. 312, p. 202.
19. Zhanpeisov, N.U., *Kinet. Catal*, 2010, vol. 51, p. 849.
20. Mattews, R.W., *J. Phys. Chem.*, 1988, vol. 92, p. 6853.
21. Sahate, J., Anderson, M.A., Kikkawa, H., Edwards, M., and Hill, G.G., *J. Catal.*, 1991, vol. 127, p. 167.
22. Yoneyama, H., Hag, S., and Yamanaka, S., *J. Phys. Chem.*, 1989, vol. 93, p. 4833.
23. Tanaka, T., Teramura, K., Yamamoto, T., Takenaka, S., Yoshida, S., and Funabiki, T., *J. Photochem. Photobiol., A*, 2002, vol. 148, p. 277.
24. Matsuda, A., Higashi, Y., Tanada, K., and Tatsumisago, M., *J. Mater. Sci.*, 2006, vol. 41, p. 8101.
25. Chao Xie, Zili Xu, Qiujing Yang, Baoyong Xue, Yaoguo Du, and Jiahua Zhang, *Mater. Sci. Eng., B*, 2004, vol. 112, p. 34.
26. Yamashita, H., Nishio, Sh., Katayama, I., Nishiyama, N., and Fujii, H., *Catal. Today*, 2006, vol. 111, p. 254.
27. Wilhelm, P., Zetzsch, C., and Stephan, D., *Prog. Colloid Polym. Sci.*, 2006, no. 133, p. 147.
28. Kalele, S., Dey, R., Hebalkar, N., Urban, J., Gosavi, S.W., and Kulkarni, S.K., *Pramana J. Phys.*, 2005, vol. 65, p. 787.
29. Murashkevich, A.N., Alisienok, O.A., Lavitskaya, A.S., and Zharskii, I.M., *Vest. Nats. Akad. Navuk Belarusi, Ser. Khim. Navuk*, 2009, no. 2, p. 16.
30. Wilhelm, P. and Dietmar, S., *J. Photochem. Photobiol., A,* 2007, vol. 185, p. 19.
31. Li, G., Bai, R., and Zhao, X.S., *Ind. Eng. Chem. Res.*, 2008, vol. 47, p. 8228.
32. Ei-Toni, A.M., Yin, Sh., and Sato, T., *J. Colloid Interface Sci.*, 2006, vol. 300, p. 123.
33. Marugan, J., Hufschmidt, D., Lopez-Munoz, M.-J., Selzer, V., and Bahnemann, D., *Appl. Catal.,* 2006, vol. 62, p. 201.
34. Murashkevich, A.N., Lavitskaya, A.S., Alisienok, O.A., and Zharskii, I.M., *Inorg. Mater.*, 2009, no. 10, p. 1146.
35. Murashkevich, A.N., Alisienok, O.A., and Zharskii, I.M., *Sviridovskie Chteniya*, Minsk, 2009, no. 5, p. 161.
36. *Refractories and Refractory Raw Materials: Methods for Determination of Titanium(IV) Oxide*, RF Standard GOST 2642.6-97.
37. Kol'tsov, S.I. and Tuz, T.V., *Izv. Vyssh. Uchebn. Zaved., Khim. Khim. Tekhnol.*, 1991, vol. 34, no. 2, p. 90.
38. Epling, G.A., *Chemosphere*, 2002, vol. 46, p. 561.
39. Tanaka, K., Padermpole, K., and Higanaga, T., *Water Res.,* 2000, vol. 34, p. 327.
40. Murashkevich, A.N., Lavitskaya, A.S., Alisienok, O.A., and Zharskii, I.M., *Sviridovskie chteniya* (Sviridov Workshop), Minsk, 2008, no. 4, p. 86.
41. Gorenberg, A.A., *Extended Abstract of Cand. Sci. (Phys.–Math.) Dissertation*, Moscow: Inst. of Chemical Physics, 2009.
42. Fedotova, M.P., *Extended Abstract of Cand. Sci.* (*Chem.*) *Dissertation*, Tomsk: Tomsk State Univ., 2009.